10.A(2)
206th CM

Received: 13 February 2024 | Accepted: 12 May 2024

DOI: 10.1111/2041-210X.14408

Methods in Ecology and Evolution
Open Access
BRITISH ECOLOGICAL SOCIETY

RESEARCH ARTICLE

Incorporating telemetry information into capture-recapture analyses improves precision and accuracy of abundance estimates given spatiotemporally biased recapture effort

Janelle J. Badger[1] | **Devin S. Johnson**[1] | **Robin W. Baird**[2] | **Amanda L. Bradford**[1] | **Michaela A. Kratofil**[2,3,4] | **Sabre D. Mahaffy**[2] | **Erin M. Oleson**[1]

[1]Pacific Islands Fisheries Science Center, NMFS, NOAA, Honolulu, Hawaii, USA

[2]Cascadia Research Collective, Olympia, Washington, USA

[3]Marine Mammal Institute, Oregon State University, Newport, Oregon, USA

[4]Department of Fisheries, Wildlife, and Conservation Sciences, Oregon State University, Corvallis, Oregon, USA

Correspondence
Janelle J. Badger
Email: janelle.badger@noaa.gov

Funding information
National Marine Fisheries Service; Marine Mammal Commission; Tides Foundation; Wild Whale Research Foundation; Office of Naval Research

Handling Editor: Miguel Acevedo

Abstract

1. Natural populations that are rare, cryptic or inaccessible provide a monumental challenge to monitoring, as adequate data are extremely difficult to collect. Surveys often encompass only a small portion of a population's range due to difficult terrain or inclement weather, especially for populations with extensive ranges. Thus, to maximise encounters, sampling efforts may be largely opportunistic or biased to accessible areas. The resulting sparse and spatially biased data may be difficult to model, standardise across years and incorporate into an assessment or management framework. However, in many monitoring programs, there are usually multiple threads of data that, though each may have its own limitations, can be synthesised to reveal important ecological processes.
2. Here, we demonstrate a simple technique to incorporate two additional streams of data on the same population, telemetry and survey effort data, into capture-recapture analyses to address spatiotemporal sampling bias using simulated data. Utilisation distributions (UDs) computed from telemetry data are overlaid with UDs of survey efforts, providing an 'effort by animal space use' overlap covariate for modelling detection in a Jolly–Seber open population model.
3. Using simulated data, we found that our method resulted in more accurate and precise estimates of abundance than traditional capture-recapture models. We then applied this method to a 16 year photo-identification capture-recapture dataset ($n = 143$ individuals) along with telemetry data ($n = 44$ satellite tag deployments) collected from the endangered population of false killer whales resident to the main Hawaiian Islands.
4. Incorporating space use and effort into this analysis improved precision of abundance estimates relative to previous modelling endeavours.

KEYWORDS
capture-recapture, data integration, false killer whales, Jolly–Seber, telemetry

1 | INTRODUCTION

Robust assessments of population abundance and trends are necessary to develop effective management strategies and monitor outcomes of conservation actions (Dobson, 2005; Nichols & Williams, 2006; Sibly & Hone, 2002). However, evaluating wild populations presents a formidable challenge to ecologists due to the logistical and financial demands of field efforts, as well as the subsequent task of fitting appropriate statistical models to estimate abundance (Lindenmayer & Likens, 2010; Reed & Blaustein, 1997; Yoccoz et al., 2001).

Particularly for rare, cryptic or inaccessible populations, survey efforts tend to have low encounter rates and may lack spatial and temporal consistency or coverage, with practical and financial hurdles to reasonably repeat surveys at a system-appropriate rate to determine trends (Dobson, 2005; Petrovskaya et al., 2012; Thompson, 2004). The resulting sparse datasets may preclude modelling of important processes and suffer from unmeasured biases, limiting power to assess abundance, extinction risk and other important metrics (Doak et al., 2005; Lesser & Brewer, 2012; Rosenbaum, 1991). When using capture-recapture (CR) methods for estimating abundance, variation in the exposure of individuals to sampling arising from this spatiotemporal bias in field efforts can obscure interpretation of estimated abundance, as it is unclear to what proportion of the population any analysis extends (Hammond et al., 2021; Marsh & Sinclair, 1989). Consequently, survey efforts are difficult to incorporate into management frameworks, which is particularly egregious in recovery plans for vulnerable populations, which may be more likely to present challenges to sampling. When CR data are collected with spatial reference, spatially explicit CR (SECR or SCR) models can theoretically be manipulated to account for varied spatiotemporal effort (Tourani, 2022), however, they require animals having relatively constrained home ranges and movement relative to the study area (Sollmann et al., 2012). Here, we present a straightforward method for incorporating auxiliary location data to account for varied spatiotemporal effort in nonspatial CR models to estimate abundance of wide-ranging species.

Conventional CR models are generally not equipped to account for the spatial and temporal bias inherent to opportunistic study designs. Some modifications have been developed to address these concerns, either as alterations to the modelling framework or in post-processing steps. For example, analysts may adjust abundance estimates by the proportion of the study area sampled in systems where it is appropriate to assume the population is uniformly distributed and remains stationary relative to survey efforts (Defeo & Rueda, 2002; Thompson, 2004). However, this method requires sufficient system knowledge to evaluate such assumptions and would not be reasonable for wide-ranging or highly mobile populations for which survey efforts can only cover a small portion of the population's range. Other methods to account for study designs that vary among sampling occasions include changes to the model structure or framework, such as estimating site- and time-specific detection probabilities in CR methods (Agresti, 1994). Further, availability bias, or heterogeneity in capture probability, cannot be modelled explicitly. Instead, it must be explained by individual covariates (if available) or approximated by classical models of latent heterogeneity such as the beta-binomial mixture model (Burnham & Overton, 1979), the logit-normal mixture (Coull & Agresti, 1999) or finite mixtures (Norris & Pollock, 1996). Estimating these additional parameters or fitting more complex models can be incredibly data-hungry, especially when analysts must also account for variation due to groupings such as sex or social group. Ultimately, such solutions are often inaccessible to researchers fitting models to sparse datasets that do not have the power to estimate additional parameters demanded by saturated or complex model structures.

While isolated data streams may prove insufficient to obtain robust estimates of population parameters, there is a rapidly growing body of work to synthesise multiple data sources to take on the task (Gardner et al., 2022; Grace et al., 2016; Hostetter et al., 2019; Schaub & Abadi, 2011; Zipkin et al., 2019; Zipkin & Saunders, 2018). Monitoring efforts often pursue multiple lines of data, and incorporating different data types into population analyses allows researchers to efficiently make use of all available information to improve resulting parameter estimates (Gardner et al., 2022; Jarrett et al., 2022; Schaub et al., 2007). For example, studies of animal abundance and distribution are often conducted independently of research on movement and space use, despite the obvious links between the processes (Morales et al., 2010). Availability of animals to survey efforts as well as spatial variation in density directly impact probability of detection and may be informed by movement data. In recent years, there has been an effort to incorporate animal telemetry data into spatially explicit capture-recapture models (see Tourani (2022) and the recent Ecology special issue highlighted by Converse et al. (2022)). SCR models account for heterogeneous detection by explicitly modelling an animal's movement about its home range and the relative exposure of its home range to detection by fixed surveys (e.g. camera traps) or other sampling (e.g. DNA sampling). In these models, animals move through a study area depending on an activity center and a dispersion parameter, which are often estimated using the locations of individual detections. SCR methods are under intensive development, for example, recent advances include integrating telemetry data to inform the dispersion parameter (McClintock et al., 2022), allowing for dynamic activity centers based on Markovian or random transience and dispersal (Royle et al., 2016), and using nonparametric methods to define the home range (Hooten et al., 2023).

Available SCR methods may not be applicable in all systems, especially those with highly mobile and elusive populations with large home ranges in inaccessible habitats (e.g. cetaceans and highly migratory species; Tourani, 2022). Heterogeneity in detection due to availability will likely occur if individual animals readily traverse across a broad range that covers a large proportion of the study area, but smaller-scale survey effort changes in location and intensity at each occasion. Individual exposure to survey effort will vary greatly at each occasion due to the changing overlap between sampling and individual space use. In this example of a highly mobile species, detection locations at each sampling occasion would not be representative of the individual's movement patterns or space use and would go so far in describing an activity center as would a random cloud of points. If the population is further a sparsely distributed, elusive species, collected capture-recapture data will be inadequate to explicitly model spatial processes within the CR modelling framework. However, extracting information on movement from available streams of data could improve models suffering from spatiotemporal bias or variability in sampling by informing availability of target populations to survey effort, without the hefty data requirements of SCR.

Many authors have developed routes to utilise ancillary movement information within non-spatial CR models. As a few examples, to account for lack of geographic closure, Ivan et al. (2013) used telemetry data to calculate the portion of the population that occurred within the boundaries of the study site to correct density estimates. Others used location data to adjust density estimates for average home range size (Balme et al., 2009; Bitetti et al., 2006; Dillon & Kelly, 2008; Sharma et al., 2010; Soisalo & Cavalcanti, 2006). However, these ad hoc corrections do not incorporate movement information relative to survey efforts directly into the process it affects, that is detection probability. We propose a simple yet effective technique to incorporate animal telemetry data into non-spatial capture-recapture models, what we refer to as a *pseudospatial* model. Our modelling structure accounts for spatiotemporal bias in survey efforts relative to animal space use to address biases in abundance estimates and other population parameters, but does not require explicit modelling of spatial processes. First, using simulated data, we compared conventional or non-spatial CR models and our pseudospatial method to determine relative performance given spatiotemporal variability in sampling. Then, we apply this method to telemetry and photo-identification data collected on an endangered population of false killer whales (*Pseudorca crassidens*) resident to the main Hawaiian Islands. Our aim is to demonstrate that this method can generate abundance estimates with improved accuracy and precision and present its utility on a rare and highly mobile population that exhibits social structure.

2 | MATERIALS AND METHODS

This multistep process includes (1) analysing animal space use data, computing population-level utilisation distribution (UD) estimates or individual-level UDs and scaling to relevant groups (e.g. social group, sex, age) to estimate population-level *animal space use*; (2) analysing spatial survey effort data, computing UD estimates for research efforts to obtain estimates of *coverage*; (3) determining availability of animals to survey coverage by finding the interaction between (1) and (2), or the *overlap*; and (4) incorporating this overlap measure within the detection process of a capture-recapture model. We will first describe these steps, then detail our simulation analysis to assess performance compared to traditional CR models, and finally apply this method to estimate abundance of a population of false killer whales in the main Hawaiian Islands, for which both capture-recapture (Bradford et al., 2018) and satellite tag (Baird et al., 2010, 2012) datasets exist.

2.1 | Determining overlap between animal space use and survey effort

Obtaining reasonable UDs for animal space use and survey effort coverage (UD_a and UD_e, subscripted ***a*** and ***e*** to denote *animal* and *effort*, respectively) can be achieved using appropriate methodology for a given data type. The UD_a should reflect population-level space use patterns for detection in survey efforts. Below, in *Application to endangered main Hawaiian Islands insular false killer whales*, we demonstrate using kernel density estimates to do so with a sample of satellite telemetry tag data and GPS tracks from survey efforts.

In many systems, detection of individuals in a CR study may have a dependency structure, such as in species that exist in social groups or clusters, or where detection varies by sex. In these cases, the individual UDs comprising UD_a should be averaged accordingly (e.g. $UD_{a,g}$ for each grouping g) so that the variation in group detection due to survey coverage can be accounted for appropriately. Likewise, if animals display temporal variability in movement and there are sufficient data to do so, UD_a may be expanded to be time-specific. Survey effort UDs should be split at the relevant temporal scale for modelling, t, such that $UD_{e,t}$ reflects the survey effort coverage for that time step.

Though there are many methods to calculate overlap between two utilisation distributions, here we compute Bhattacharyya's affinity BA (Bhattacharyya, 1943):

$$BA_{a,e} = \int_x \int_y \sqrt{UD_a(x,y)} \times \sqrt{UD_e(x,y)},$$

where $UD_a(x,y)$ and $UD_e(x,y)$ are the UD values of the animals and survey effort, respectively, at the point (x,y).

2.2 | Incorporating overlap into capture-recapture models

This overlap variable can be incorporated into capture-recapture models as a covariate in the detection process. Here we will demonstrate using a state-space formulation of the Jolly–Seber (JS) open population model to estimate abundance (Jolly, 1965; Seber, 1965; see Kéry & Schaub, 2012 for further information). Individuals can be in one of three possible states: 'not yet entered', 'alive', and 'dead' within a state vector $z_{i,t}$ for each individual i and time step t, reflected as a 1 for individuals in state 'alive' and 0 for states 'not yet entered' and 'dead'. Transitions among these states is governed by two ecological processes: entry and survival.

Suppose we have an augmented population of M individuals, of which N are genuine and $M-N$ are pseudo-individuals (Kéry &

Schaub, 2012). Entry from M to N is described using ψ, the removal entry probability, that is, the probability that governs movement from state 'not yet entered' to the state 'alive'. The state of individual i at the first occasion is determined by a Bernoulli trial with probability ψ at the first time step:

$$z_{i,1} \sim \text{Bernoulli}\left(\psi_1\right).$$

Subsequent states are determined either by survival ϕ for an individual already entered $\left(z_{i,t} = 2\right)$ or by entry, ψ_t, for those that have not $\left(z_{i,t} = 1\right)$.

Thus, the state process is

$$z_{i,t+1} \mid z_{i,t}, \ \dots, z_{i,1} \sim \text{Bernoulli}\left(z_{i,t} \times \phi_{i,t} + \psi_{t+1} \prod_{k=1}^{t} \left(1 - z_{i,k}\right) \right).$$

The observation process conditions on the state process,

$$y_{i,t} \mid z_{i,t} \sim \text{Bernoulli}\left(z_{i,t} \times p_{i,t}\right),$$

where $p_{i,t}$ is the probability of detecting individual i at time t given it has entered the population, and $\text{logit}\left(p_{i,t}\right) = \mu_t + \delta \times BA_{a,e}$, with intercepts μ_t, and $\mu_1 = \mu_2$ for identifiability.

Note that in this example, we are assuming that entry and detection are time-variant and survival is constant. Fully time-varying models require further constraints for confounding variables (Gimenez et al., 2003). Then, population abundance in a given year N_t is defined as the number of individuals in the 'alive' state, $N_t = \sum_i^M \left(z_{i,t}\right)$.

2.3 | Simulation

In order to test whether this pseudospatial JS model generates abundance estimates with greater accuracy and precision compared to the more traditional model, we simulated animal movements, survey effort, and resulting capture histories for a system in which animal space use varied among social groups and survey effort covered only a portion of the populations range and varied nonrandomly over time. We considered a population of 300 individuals composed of three social groups, with 100 individuals in each social group. Starting locations for group-level movements and 10 time steps of survey effort were chosen at random, and subsequent movement and survey tracks were modelled as correlated random walks (using package adehabitatLT v. 0.3.26, Calenge, 2006). We simulated animal tracks to have a greater degree of concentration for the wrapped normal distribution of turning angles than survey effort tracks, as survey efforts can tend to exhibit more tortuous, search-oriented behaviour than wide-ranging animals. For each of 10 time steps, surveys would detect individuals with detection probability α if they were <2 km from the survey vessel. The resulting capture histories were then fit to a conventional JS open population model and the pseudospatial JS model outlined above in a Bayesian framework. Six simulated individuals from each group were telemetered, and their locations used to estimate the group-level utilisation distributions for which survey overlap was determined.

We considered two complications: time-varying group-level space use and low detectability. Time-varying group-level space use was manipulated via a starting location that was either static over the time series or time-variant, so the small sample of individuals tagged over the course of the study may not provide an adequate characterisation of space use. Detectability varies between low, $\alpha = 0.2$, resulting in a sparse dataset, or high, at $\alpha = 0.8$.

This procedure was repeated 30 times per set of conditions (high vs. low detectability, static vs. varying group space use) to observe the range of probabilistic outcomes in capture histories. For each model, we report the difference in posterior precision (SD), the number of inaccurate abundance estimates (see below), and the proportion of iterations whose abundance estimates exhibit an inaccurate trend. We define an inaccurate abundance estimate as one where the 90% credible interval (CRI) of the posterior distribution did not contain the true population size. To detect inaccurate trends, we regressed derived abundance estimates over time for each iteration of the Bayesian Markov chain Monte Carlo (MCMC), and defined an inaccurate trend if the 90% credible interval of the resulting slope parameter distribution was distinct from 0, as abundance should be static across the time series.

2.3.1 | Model fitting and selection

A Bayesian framework was used for model fitting, selection and inference using the software JAGS 4.2.0 through the R interface rjags (R version 4.2.2; Plummer, 2003, 2018; R Core Team, 2020). We used priors that are generally uninformative, namely Uniform(0,1) priors, for probabilistic parameters constrained to [0,1]. The parameter describing the effect of overlap, δ, was given a diffuse Normal(0,1000) prior.

MCMC was used to sample the posterior distributions of the parameters of interest. For each model, we ran three chains with different sets of initial values. The first 10,000 MCMC samples were discarded as the burn-in after checking that convergence was satisfactory. Convergence of chains to stationary distributions was visually evaluated using sample path plots in conjunction with the Brooks–Gelman–Rubin diagnostic $\hat{r}$ (Brooks & Gelman, 1998), with values close to 1.00 indicating adequate convergence. Chains were then run for 20,000 iterations after burn-in, and every tenth iteration was retained for a total of 2000 MCMC samples used for inference. We determined that the overlap variable had an effect if a 95% credible interval of the posterior distribution of δ did not include 0. We assessed support for inclusion of overlap using a measure of out-of-sample predictive ability of each model, the widely applicable information criterion (WAIC, Watanabe, 2010), where a model with a smaller WAIC is judged a better fit. These Bayesian modelling methods were also applied to the empirical data, described below.

2.4 | Application to endangered main Hawaiian Islands insular false killer whales

The endangered resident population of false killer whales in the main Hawaiian Islands (MHI) provides a motivating platform to investigate methods to alleviate sampling bias concerns. This insular population is small (most recently estimated at 167 ± 23 individuals, Bradford et al., 2018), and individuals are highly mobile and frequently move among island areas (spanning the entire MHI, Baird et al., 2012; Mahaffy et al., 2023), making them sparse throughout their range. This population is known to preferentially associate in social groups, hereafter referred to as 'clusters' (Baird et al., 2008; Mahaffy et al., 2023), and there is some evidence for cluster-specific space use patterns (Baird et al., 2012). When encountered during survey efforts, individuals and subgroups of the same social cluster are often spread out, travelling kilometres apart (Baird, 2016; Baird et al., 2008, 2010, 2012). The MHI insular population of false killer whales has declined in recent decades, likely due to interactions with fisheries, and was officially designated as Endangered under the US Endangered Species Act in 2012 (Oleson et al., 2010).

Numerous aerial and boat-based surveys, photo-identification, satellite-telemetry and genetic studies have made the MHI insular population the world's most thoroughly studied population of false killer whales (Baird, 2016). However, each of these data streams presents unique difficulties in estimating necessary metrics to monitor this endangered population, such as abundance and population growth rate. For example, there is variable survey effort among the island areas of the MHI, and as this population is wide-ranging, these surveys will only encompass a small proportion of the population's range on any given trip. Weather and sea conditions generally further restrict areas viable for visual sampling on a smaller scale; surveys almost exclusively conducted on leeward sides of islands protected from trade winds (Baird et al., 2013). Differential space use by social groups and the biased nature of sampling could result in poor estimates of population abundance and trend.

While substantial work has been done to estimate abundance for this population (Bradford et al., 2018), conventional CR models cannot appropriately account for known spatiotemporal variation and bias in sampling. As it is unclear to what proportion of the population any analysis extends in any given year, resulting abundance estimates are difficult to interpret and incorporate into recovery plans. To demonstrate how our pseudospatial model may address these concerns, we fit one of the datasets used in Bradford et al. (2018) to our pseudospatial model, assuming the same social structure identified at the time of Bradford et al. (2018) (3 social clusters), and compared these results to those generated from the conventional POPAN-formulated Jolly–Seber fit in Bradford et al. (2018).

2.4.1 | Data collection

Data used in this analysis were sourced from dedicated nonsystematic surveys conducted by Cascadia Research Collective (CRC) from 2000 to 2015 (Figure 1) as part of an intensive research effort involving small boat surveys of odontocetes (i.e. toothed whales and dolphins). While CRC has undertaken surveys off all island areas within the MHI, not every area is surveyed every year, with most of the effort undertaken off of Hawaiʻi Island (Baird et al., 2013). Generally, between 1 and 6 occasions of such efforts lasting 1–6 weeks were conducted throughout each year, with surveyed areas designed to maximise likelihood of animal encounter (details of the field operations are provided in Baird et al., 2013). Even with this focused sampling, false killer whales are only encountered in about 4% of surveys. While on effort, CRC recorded location via an affixed GPS at 5-min intervals. In total, from 2000 to 2015, CRC completed 6710 on-effort hours over 927 days traversing 108,216 km resulting in 41 MHI false killer whale group sightings.

At each false killer whale sighting, researchers took photographs for individual identification based on the prevalence of permanent markings (e.g. nicks, notches) on the leading and trailing edge of the dorsal fin. For further details on the processing of these photographs, see Baird et al. (2008). In total, CRC's efforts from 2000 to 2015 resulted in a longitudinal photo-identification ('photo-ID') dataset of 143 individuals with distinctive markings visible in high-quality photographs that can be translated into encounter histories for use in CR models (details of this process can be found in Bradford et al., 2018; Figure 2) to allow for comparison to the analysis in Bradford et al. (2018). These individuals were assigned to 1 of 3 identified social clusters using the analysis of network modularity explained in Baird et al. (2012). Encounter data were compiled at an annual scale; individuals were recorded as encountered or not encountered each year. Tagging and photography was authorised under NMFS Scientific Research Permits 926, 731-1509, 731-1774, 20605, and 15330 issued to CRC. Tagging protocols and procedures were approved by the Cascadia Research Collective Institute of Animal Care and Use Committee.

When crew expertise, ocean conditions and animal behaviour allowed, research efforts also involved the deployment of satellite tags (Baird et al., 2010, 2023). Between 2007 and 2021, whales were tagged using location-only satellite tags (SPOT-5 or SPOT-6, Wildlife Computers) or location-and-dive behaviour- transmitting satellite tags (SPLASH10 or SPLASH10-F (Fastloc®-GPS), Wildlife Computers) in the Low-Impact Minimally-Percutaneous External-electronics Transmitter (LIMPET) configuration (Andrews et al., 2008). Telemetry tagging was undertaken under relevant permits from the National Marine Fisheries Service (NMFS), and tagging methods were approved by the Institutional Animal Care and Use Committees of CRC and the NMFS Pacific Islands Fisheries Science Center (PIFSC). Tags were deployed with a pneumatic projector and were attached to the dorsal fin or just below the fin of the whales by two 6.7 cm titanium darts with backward facing petals. Tags were duty-cycled to only transmit during the hours with the highest probability of a satellite being overhead. Tag transmission schedules varied by tag type and by year.

Prior to analyses, location data were filtered through the Douglas–Argos Filter (Douglas et al., 2012; via Movebank, Kranstauber et al., 2011) to remove unrealistic locations based on

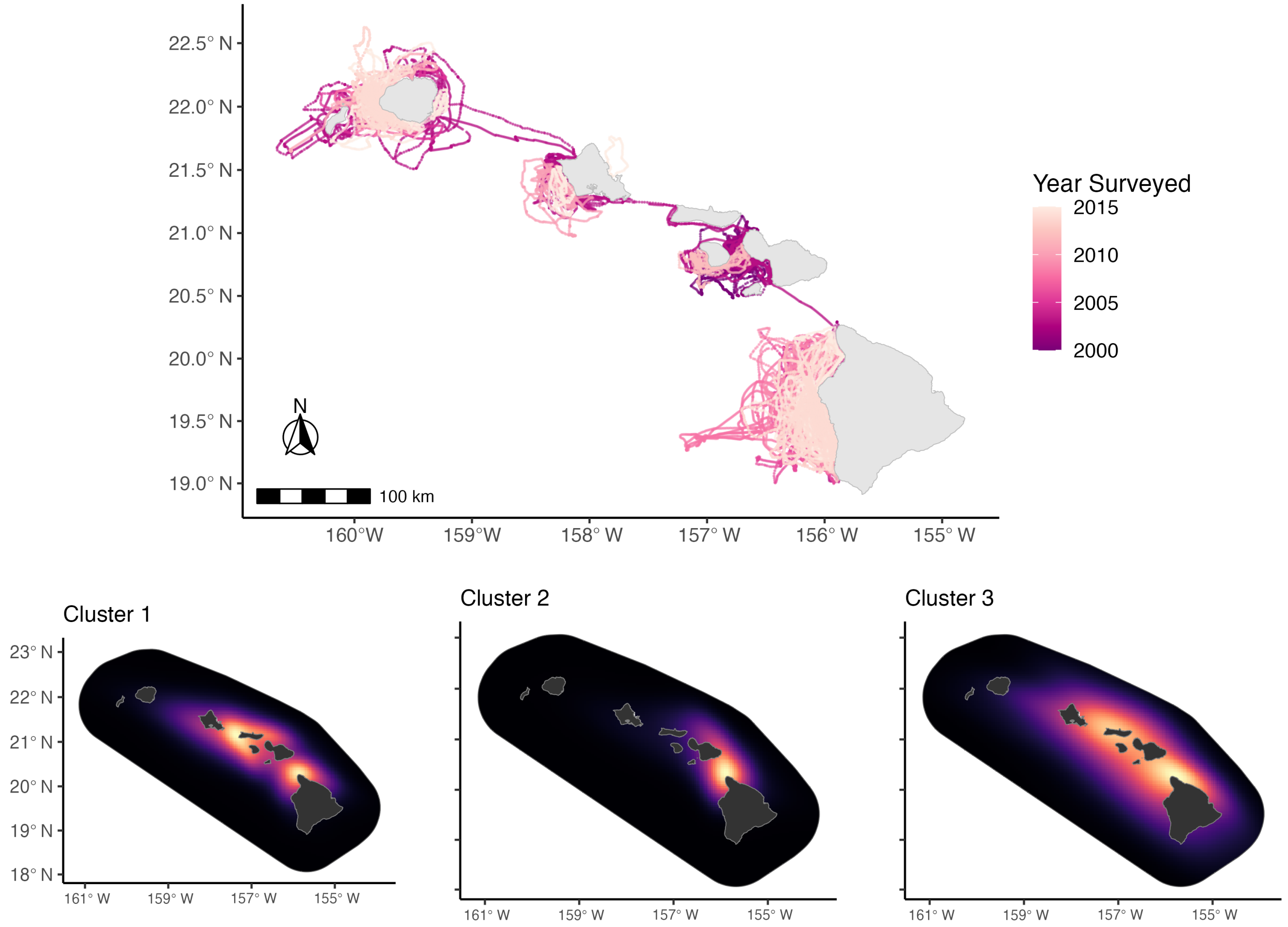

FIGURE 1 (Top) Small boat tracks from odontocete surveys conducted by Cascadia Research Collective from 2000 to 2015 in the main Hawaiian Islands. Black line indicates population boundary (Bradford et al., 2015). Colour represents survey year, in continuous scale with darker colours indicating earlier years of the time series. (Bottom) Left to right, depicts in order the cluster-level space use of main Hawaiian Islands insular false killer whales determined from kernel density estimators of location data from 44 tags deployed on individuals from the three social clusters from 2007 to 2021.

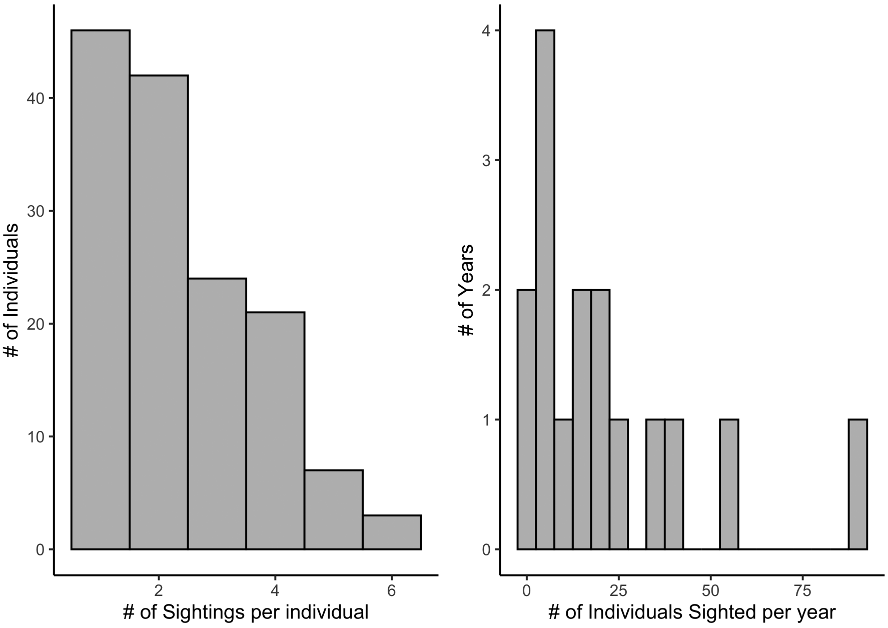

FIGURE 2 Summary information for false killer whale group sightings over 16 years (2000–2015), comprised of 143 individuals.

travelling speeds and turning angles, using settings defined in Baird et al. (2012). Fastloc-GPS locations for relevant tag deployments ($n=2$) were filtered by removing locations with residual values greater than 35 and time errors greater than 10 s (Dujon et al., 2014) and subsequently running the data through a general speed filter via Movebank (Kranstauber et al., 2011). When applicable, one of each pair of tagged individuals moving in concert were removed prior to analyses to reduce pseudoreplication (see Schorr et al., 2009 for details). The resulting dataset included 44 deployments (Cluster 1, $n=31$; Cluster 2, $n=4$; Cluster 3, $n=9$), ranging from 12 to 199 days of data (mean = 62.5/median = 48.8) that were analysed for population-level space use (Figure 1).

2.4.2 | Model form and fitting

Analysing animal telemetry data

First, for each telemetered false killer whale, locations were fit to a continuous-time correlated random walk (CTCRW) model using the R package crawl (v. 2.2.1, Johnson et al., 2008) to account for location error and predict locations (paths) from observed animal locations. These imputed paths were rerouted around impenetrable terrain features (i.e. land) using the R package pathroutr (London, 2020). Then individual utilisation distributions were described using a kernel density estimator (KDE) in the R package ks (Duong, 2007). For the KDE estimator, we use a simple plug-in band-width h_i equal to,

$$h_i = n_{ei}^{-1/3} \times \Sigma_i,$$

where Σ_i is the covariance matrix among locations for the ith individual, and n_{ei} is the effective sample size (ESS) of the ith individual's telemetry dataset (Bartoszek, 2016). The ESS uses the correlation structure of the CTCRW model to determine the effective number of observations that will be less than the total number of observed locations that will inflate the kernel size. This approach is similar to the autocorrelated kernel density estimate of Fleming et al. (2015) in that it seeks to produce a more predictive UD that accounts for the limited time observation of an animal's correlated travel. The full form of the kernel density estimator for the ith telemtered individual, $\hat{f}_i$, is given below.

Let $(s_1, \ldots, s_n)$ be telemetry locations, such that $s_j = \{x_j, y_j\}$ where x_j and y_j are coordinates in each cardinal direction, $j \in \{1, \ldots, n_i\}$, and n_i is the total number of locations for the ith individual

$$\hat{f}_i = \frac{1}{n_i \times h_i} \sum_{j=1}^{n_i} K\left(\frac{s - s_j}{h_i}\right),$$

where K is a Gaussian kernel, that is $K(u) = \frac{1}{\sqrt{2\pi}} e^{-\frac{1}{2}u^2}$. The resulting f_i were then normalised to sum to 1 over the study area.

The resulting UD provides a density surface for individual presence in space; however, in order to use the telemetry data information for non-telemetered animals in the CR population, we provide an estimate of *population*-level space use to determine animal availability to our survey efforts. As these island-associated false killer whales are known to be affiliated as stable distinct social groups or clusters, individual UDs were averaged by social cluster membership (Figure 3), henceforth referred to as $UD_c(s) = \text{mean}_i(f_i(s))$, which is subscripted c to denote *cluster*. There are many ways we might weight individual UDs when averaging (see Conn et al., 2022); however, as we aimed to develop an overall use index, we used the straight average UD.

Though the CR dataset is filtered to 2000–2015, we included all available tag data (2007–2021) to inform the cluster-level utilisation distributions. We assume, in our choice to use all available data and estimate a time-invariant cluster UD, that the greatest source of variation in movement patterns is due to cluster membership and that cluster membership is fixed and individuals do not switch clusters. While it is unlikely that cluster-specific space use for this population has remained entirely stationary over 15 years, sample sizes for each cluster inhibit our ability to estimate time-specific UDs.

Analysing survey effort GPS data

Effort data including timestamps and locations, such as tracks via an affixed GPS in the case of the false killer whale survey effort data, can be analysed similarly. We compute survey effort coverage using a simple kernel density estimate of survey tracks from each year, subsequently referred to as $UD_{e,t}$ for $t \in \{1, \ldots, T\}$, where T is the

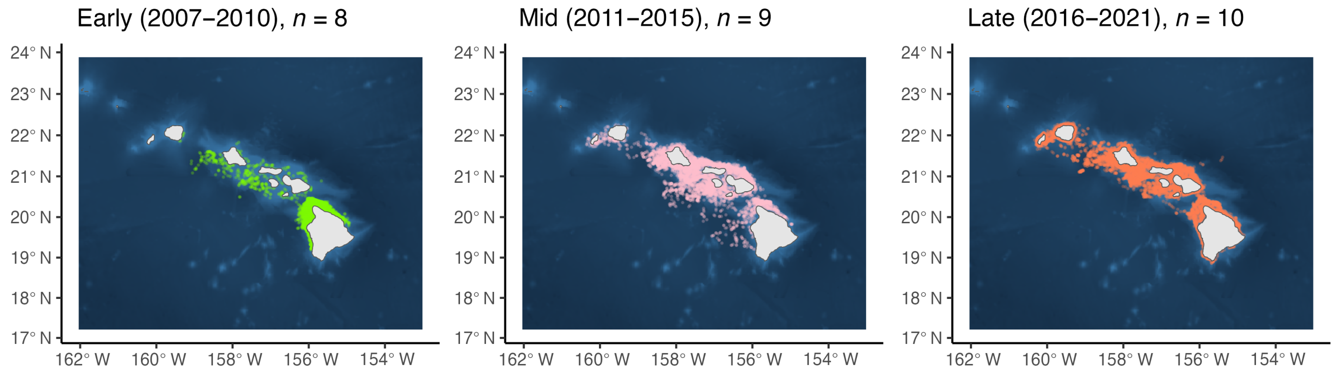

FIGURE 3 Location data from Cluster 1 false killer whales in the Main Hawaiian Islands over the time series, split into early, mid- and late periods to depict temporal variation in cluster space use.

data time series length. Bandwidth should be platform-specific, here based on the average sighting distance from survey vessels of about 1.5 km (Baird et al., 2013).

2.4.3 | Incorporating overlap into CR model

We accounted for the lack of independence from social cluster in the detection process. After computing the overlap of the cluster UDs with time-specific survey effort, the resulting overlap measurements were both time- and cluster-specific (Figure 4). Estimating cluster-by-time interaction terms for detection parameters within a CR model requires rich data, and our method is effectively equivalent, costing only one additional parameter. However, we must assume that the greatest source of variation in cluster detection is overlap with survey efforts. The conventional CR model used in Bradford et al. in 2018 simply estimated varying intercepts by cluster. The model for the detection process was

$$\text{logit}\left(p_{i,t}\right) = \mu_t + \delta \times \text{overlap}_{t,c_i},$$

where μ is the intercept, c refers to the cluster assignment of individual i, and t refers to time step. The covariate $\text{overlap}_{t,c_i}$ refers to the standardised Bhattacharyya's affinity BA overlap for each cluster $BA_{c,e,t}$ measure over time, that is $\text{overlap}_{c,t} = \frac{BA_{c,e,t} - \mu}{\sigma}$, where $\mu = \frac{1}{T}\sum_1^T BA_{c,e,t}$ and $\sigma = \sqrt{\frac{\Sigma\left(BA_{c,e,t} - \mu\right)^2}{T}}$.

For comparison of estimability, we also fit models with interactive cluster and time effects, such that the detection process becomes:

$$\text{logit}\left(p_{i,t,c}\right) = \mu_{t,c}.$$

Priors for $\text{logit}^{-1}\mu$ and entry probability ψ_t were given uninformative Uniform(0,1) distributions, but previous analyses and expert knowledge of life history of this species (i.e. long-lived) indicate high survival, so we used an informative Beta(8,1) prior for the temporally constant ϕ.

Importantly, using photo-ID for CR analyses allows us to only estimate the number of distinctive individuals, as nondistinctive individuals will never be 'resighted' and included in our dataset. About 25% of individuals in sighted groups are nondistinctive, though this varies by year and group. Estimates of N_t here correspond to the number of distinctive individuals present in the population in the given year. Though not included in this analysis, this value would typically be adjusted for an estimated proportion distinctive from group sightings in post-processing (see Bradford et al., 2018).

3 | RESULTS

3.1 | Simulation experiment

The results from testing the pseudospatial model on simulated mark-resight and telemetry data demonstrated that, overall, including the overlap covariate in the detection process substantially improves accuracy of posterior distributions of derived population size and population trend (Table 1). The pseudospatial model was especially effective when animal space use patterns were consistent over time and thus well-characterised, but still performed marginally better than the conventional model when these conditions were not met. If space use were constant and encounters common, the pseudospatial model accurately estimated population size and trajectory 93% and 88% of the time, versus conventional models at 87% and 81%, respectively.

3.2 | Application to main Hawaiian Islands insular false killer whales

We fit the conventional JS model and the pseudospatial JS model to the main Hawaiian Islands false killer whale photo-ID data and found

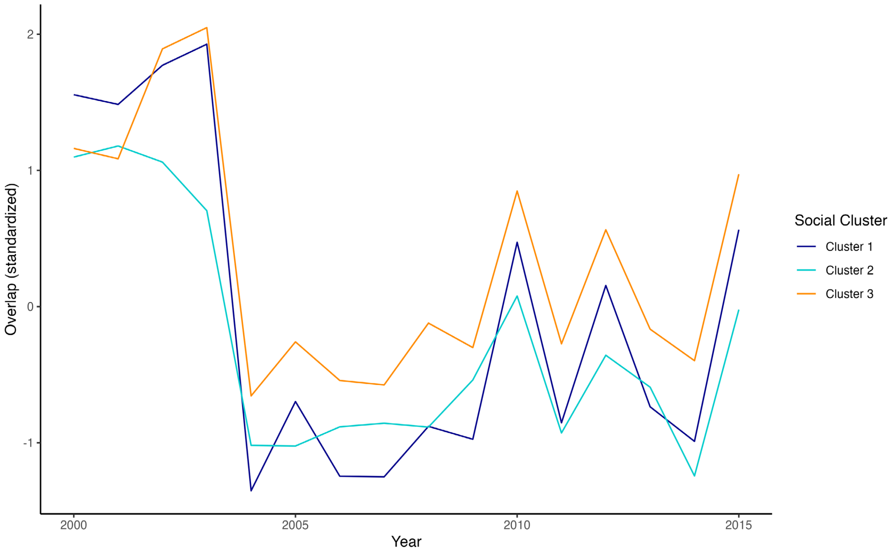

FIGURE 4 Overlap of survey efforts by Cascadia Research Collective and social cluster-level space use of the main Hawaiian Island insular false killer whale population from 2000 to 2015, calculated using Bhattacharyya's affinity.

a strong preference for the pseudospatial JS model (ΔWAIC = 26.7, Figure 5). Models including an interactive effect of cluster and time failed to converge, and even parameters with $\hat{r}$ near the conventionally acceptable maximum (1.1) had diffuse posterior distributions. Posterior density of δ, the parameter describing the effect of overlap on detection probability, was distinctly positive, such that surveys with greater coverage of cluster-level space use had greater probability of encountering false killer whales. The inclusion of the overlap of animal space use and survey efforts allowed for greater precision in posterior distributions of yearly estimated number of distinctive individuals (Figure 5). The pseudospatial model estimated these derived quantities with, on average, 1.68× greater precision than the conventional model. Throughout the time series, the pseudospatial model point estimates of distinctive individuals were marginally greater than conventional model, though 95% credible intervals overlap, indicating these estimates are not statistically distinct.

TABLE 1 Performance of the pseudospatial and conventional Jolly–Seber open population model fit to 30 simulated datasets under varying conditions.

	Conventional/pseudospatial	
	Encounters rare	**Encounters common**
% with true N		
Space use constant	76%/90%	87%/93%
Space use variable	75%/78%	86%/91%
% with true trend		
Space use constant	67%/78%	81%/88%
Space use variable	62%/67%	70%/74%
Increase in posterior precision, mean (conventional σ/pseudospatial σ)		
Space use constant	1.89	1.67
Space use variable	1.09	1.07

Note: % with true *N* and % with true trend refer to the accuracy (90% CRI) of posterior distributions of abundance and the slope parameter in a regression fit to yearly abundance estimates.

4 | DISCUSSION

Here we demonstrate a simple method for accounting for spatiotemporal variation in sampling that affects animal availability in survey efforts. Our simulation results show that models including the overlap between survey efforts and animal space use provide greater accuracy and precision in estimating abundance and population trend. Where simultaneous re-sight and space use data are available, this method can be used to obtain robust estimates of population abundance even for sparse datasets on rare and elusive species.

For populations such as endangered false killer whales in the MHI, spatiotemporal variation in survey efforts has rendered estimates from conventional models that are difficult to interpret. As this population is subdivided into a number of discrete social groups (Baird et al., 2012; Mahaffy et al., 2023; Martien et al., 2019), the variation in areas of their range that are surveyed in any given year induces a cluster-by-time effect on probability of detection. We fit models that accounted for an additive cluster and time-varying detection but estimation of the parameters involved in the interactive effect was strained due to the sparse resight data, with high uncertainty and low agreement among Markov chains. Assuming cluster-level movements are well-characterised by our telemetry sample, our technique sufficiently accounts for the cluster-by-time effect using telemetry data. For this population, the pseudospatial model estimated abundances that were more precise and slightly greater than the conventional JS model (Figure 5). This discrepancy is to be expected; because the conventional model does not account for the partial sampling of the study area each year, we expect the resulting estimates of population size in any given year to be biased low (Bradford et al., 2018). Capture heterogeneity of any kind is known to be associated with underestimates of population size when using

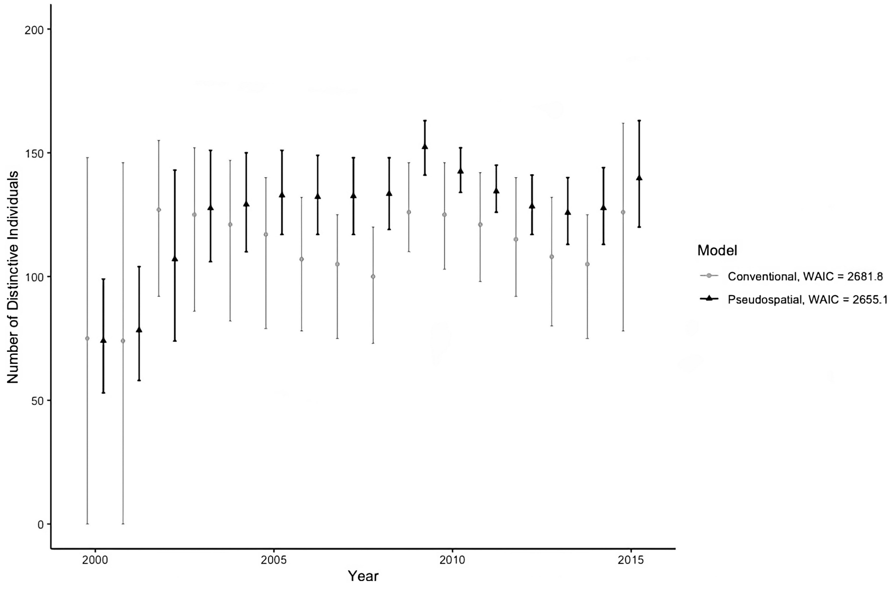

FIGURE 5 Abundance estimates of distinctive MHI insular false killer whales, 2000–2015, from the conventional Jolly–Seber population model (grey) as fit to CRC data by Bradford et al. (2018), and the pseudospatial Jolly–Seber model (black) fit to those same data. Points and bars represent posterior means and 95% credible intervals, respectively.

the Jolly–Seber model (Carothers, 1973). Incorporating telemetry data into abundance estimation will greatly aid recovery metric accuracy and power to detect trends but can also bolster stakeholder confidence in management outcomes for this population.

Generally, the relative performance of this method relies on how well movement patterns and space use of target population are characterised, that is, the animals sampled with telemetry are representative of the animals in the target population. Due to the lack of available data on MHI false killer whales, this means that we are limited to assume that cluster-level space use has remained reasonably consistent over the time series. Previous analyses of visual and tag data show spatial partitioning among social clusters that appear to be consistent over time (Baird et al., 2008, 2021; Figure 3) and genetic and capture-recapture data show that these clusters are stable over time (Mahaffy et al., 2023; Martien et al., 2019). Limited tag deployment sample size from the three social clusters precluded us from estimating time-specific space use kernels. Further, we assume that variation in individual space use patterns is mostly explained by social cluster membership, and any variation due to variables such as sex, life stage, and individual is minimal. Variation in the physical environment may also play an influential role in their space use patterns, although such variation is not expected to influence the scale of space-use considered here (i.e. yearly). We did explore the effect of poorly characterised space use patterns on model performance in our simulation and found that the pseudospatial model performed marginally better than the conventional model even with temporal changes in social group space use. Therefore, we can be relatively confident that we are not inducing additional bias and reducing the quality of the estimates below that of the traditional JS model. When space use is not well-characterised, the model may still benefit from the UD describing some variation due to survey effort, as the survey effort UD is not normalised. Future simulations may explore other forms of variation in movement patterns that may affect model performance, as well as different population trends, sizes, disparate group abundances and accuracy in model parameter estimates (e.g. detection error, survival).

The improvement in model performance with the incorporation of information on space use (from telemetry data) here follows that of previous work with spatial capture-recapture tools, while avoiding distributional assumptions about activity centers or movement parameters and complex modelling frameworks. It is, therefore, generally, more accessible to non-experts. Our simple, novel method is generalisable to many different biological systems for which simultaneous animal space use and survey data exist and can be implemented in any inferential method that accounts for imperfect detection. Incorporating the relationship between animal movement and survey effort in the estimation of abundance makes effective use of available data and holds promise as a framework for monitoring and assessing wildlife populations.

AUTHOR CONTRIBUTIONS

Janelle J. Badger and Devin S. Johnson conceived the work with significant input from Amanda L. Bradford, Michaela A. Kratofil, Erin M. Oleson and Robin W. Baird. Statistical analysis was completed by Janelle J. Badger and Devin S. Johnson. Data collection, processing and packaging was completed by Sabre D. Mahaffy, Michaela A. Kratofil and Robin W. Baird. Janelle J. Badger drafted the manuscript with contributions and revisions from all authors.

ACKNOWLEDGEMENTS

Data used in this analysis were part of a long-term study made possible by multiple grants and contracts from NOAA Fisheries and US Navy (LMR, ONR, and Pacific Fleet) to Cascadia Research Collective, as well as support from the Tides Foundation, the Marine Mammal Commission, and by the Wild Whale Research Foundation. A myriad of team members, both staff and volunteers, contributed to CRC's long-term odonotcete research, and we would like to in particular thank Annie Gorgone for early contributions to CRC's false killer whale catalogue. Photos were collected under NMFS permits 774-1437, 774-1714 and 14097 (issued to SWFSC), 20311 and 15420 (issued to PIFSC), and 20605 (issued to CRC), and under NMFS Scientific Research Permits 926, 731-1509, 731-1774 and 15330 issued to CRC. We thank Erik Franklin and Mark Miller for previous discussions that informed this analysis, as well as two anonymous reviewers and Jason Baker for their technical and editorial insights that greatly improved this manuscript.

CONFLICT OF INTEREST STATEMENT

The authors declare no conflict of interest.

PEER REVIEW

The peer review history for this article is available at https://www.webofscience.com/api/gateway/wos/peer-review/10.1111/2041-210X.14408.

DATA AVAILABILITY STATEMENT

Code and summarised data (encounter histories, utilisation distributions) that can be used to run this analysis can be found at https://github.com/badgerjj/pseudospatialCR and archived via Zenodo https://zenodo.org/records/12748573 (Badger, 2024). The raw telemetry data from which these data were made are available at the Animal Telemetry Network (Baird, 2024).

ORCID

Janelle J. Badger https://orcid.org/0000-0001-5927-7301
Devin S. Johnson https://orcid.org/0000-0002-0068-7098
Robin W. Baird https://orcid.org/0000-0002-9419-6336
Amanda L. Bradford https://orcid.org/0000-0002-3236-834X
Michaela A. Kratofil https://orcid.org/0000-0001-9519-9152
Sabre D. Mahaffy https://orcid.org/0000-0001-8255-192X
Erin M. Oleson https://orcid.org/0000-0002-4889-6059

REFERENCES

Agresti, A. (1994). Simple capture-recapture models permitting unequal catchability and variable sampling effort. *Biometrics*, *50*, 494–500.

Andrews, R. D., Pitman, R. L., & Ballance, L. T. (2008). Satellite tracking reveals distinct movement patterns for type b and type c killer whales in the southern ross sea, Antarctica. *Polar Biology*, *31*, 1461–1468.

Badger, J. (2024). *badgerjj/pseudospatialCR: Release v11.0*.

Baird, R. (2024). *Odontocete tagging in the main Hawaiian Islands, 2007–2024*. https://portal.atn.ioos.us/#metadata/1f1ff520-a4f5-4425-9681-57396059f1c9/project

Baird, R. W. (2016). *The lives of Hawai'i's dolphins and whales: Natural history and conservation*. University of Hawai'i Press.

Baird, R. W., Anderson, D. B., Kratofil, M. A., & Webster, D. L. (2021). Bringing the right fishermen to the table: Indices of overlap between endangered false killer whales and nearshore fisheries in Hawai'i. *Biological Conservation*, *255*, e108975.

Baird, R. W., Cornforth, C. J., Mahaffy, S. D., Lerma, J. K., Harnish, A. E., & Kratofil, M. A. (2023). Field studies and analyses from 2020 through 2022 to support the cooperative conservation and long-term management of main Hawaiian islands insular false killer whales. *Report to the State of Hawai'i Board of Land and Natural Resources under Contract No. 68819*.

Baird, R. W., Gorgone, A. M., McSweeney, D. J., Webster, D. L., Salden, D. R., Deakos, M. H., Ligon, A. D., Schorr, G. S., Barlow, J., & Mahaffy, S. D. (2008). False killer whales (*Pseudorca crassidens*) around the main Hawaiian islands: Long-term site fidelity, inter-Island movements, and association patterns. *Marine Mammal Science*, *24*, 591–612.

Baird, R. W., Hanson, M. B., Schorr, G. S., Webster, D. L., McSweeney, D. J., Gorgone, A. M., Mahaffy, S. D., Holzer, D. M., Oleson, E. M., & Andrews, R. D. (2012). Range and primary habitats of Hawaiian insular false killer whales: Informing determination of critical habitat. *Endangered Species Research*, *18*, 47–61.

Baird, R. W., Schorr, G. S., Webster, D. L., McSweeney, D. J., Hanson, M. B., & Andrews, R. D. (2010). Movements and habitat use of satellite-tagged false killer whales around the main Hawaiian islands. *Endangered Species Research*, *10*, 107–121.

Baird, R. W., Webster, D. L., Aschettino, J. M., Schorr, G. S., & McSweeney, D. J. (2013). Odontocete cetaceans around the main Hawaiian islands: Habitat use and relative abundance from small-boat sighting surveys. *Aquatic Mammals*, *39*, 253–269.

Balme, G. A., Hunter, L. T. B., & Slotow, R. (2009). Evaluating methods for counting cryptic carnivores. *Journal of Wildlife Management*, *73*, 433–441.

Bartoszek, K. (2016). Phylogenetic effective sample size. *Journal of Theoretical Biology*, *407*, 371–386. https://www.sciencedirect.com/science/article/pii/S002251931630159X

Bhattacharyya, A. (1943). On a measure of divergence between two statistical populations defined by their probability distributions. *Bulletin of the Calcutta Mathematical Society*, *35*, 99–109.

Bitetti, M. S. D., Paviolo, A., & Angelo, C. D. (2006). Density, habitat use and activity patterns of ocelots (*Leopardus pardalis*) in the Atlantic forest of Misiones, Argentina. *Journal of Zoology*, *270*, 153–163.

Bradford, A. L., Baird, R. W., Mahaffy, S. D., Gorgone, A. M., McSweeney, D. J., Cullins, T., Webster, D. L., & Zerbini, A. N. (2018). Abundance estimates for management of endangered false killer whales in the main Hawaiian islands. *Endangered Species Research*, *36*, 297–313.

Bradford, A. L., Oleson, E. M., Baird, R. W., Boggs, C. H., Forney, K. A., & Young, N. C. (2015). Revised stock boundaries for false killer whales (*Pseudorca crassidens*) in Hawaiian waters. U.S Dep. Commerc. NOAA Tech Memo. NOAA-TM-NMFS-PIFSC-47 (p. 29).

Brooks, S. P., & Gelman, A. (1998). General methods for monitoring convergence of iterative simulations. *Journal of Computational and Graphical Statistics*, *7*, 434–455.

Burnham, K. P., & Overton, W. S. (1979). Robust estimation of population size when capture probabilities vary among animals. *Ecology*, *60*, 927–936.

Calenge, C. (2006). The package adehabitat for the r software: Tool for the analysis of space and habitat use by animals. *Ecological Modelling*, *197*, 1035–1519.

Carothers, A. D. (1973). The effects of unequal catchability on Jolly–Seber estimates. *Biometrics*, *29*, 79–100.

Conn, P. B., Hoef, J. M. V., McClintock, B. T., Johnson, D. S., & Brost, B. (2022). A glmm approach for combining multiple relative abundance surfaces. *Methods in Ecology and Evolution*, *13*, 2236–2247.

Converse, S. J., McClintock, B. T., & Conn, P. B. (2022). Special feature: Linking capture–recapture and movement. *Ecology*, *103*, 1–3.

Coull, B. A., & Agresti, A. (1999). The use of mixed logit models to reflect heterogeneity in capture- recapture studies. *Biometrics*, *55*, 294–301.

Defeo, O., & Rueda, M. (2002). Spatial structure, sampling design and abundance estimates in sandy beach macroinfauna: Some warnings and new perspectives. *Marine Biology*, *140*, 1215–1225.

Dillon, A., & Kelly, M. J. (2008). Ocelot home range, overlap and density: Comparing radio telemetry with camera trapping. *Journal of Zoology*, *275*, 391–398.

Doak, D. F., Gross, K., & Morris, W. F. (2005). Understanding and predicting the effects of sparse data on demographic analyses. *Ecology*, *86*, 1154–1163.

Dobson, A. (2005). Monitoring global rates of biodiversity change: Challenges that arise in meeting the convention on biological diversity (CBD) 2010 goals. *Philosophical Transactions of the Royal Society, B: Biological Sciences*, *360*, 229–241.

Douglas, D. C., Weinzierl, R., Davidson, S. C., Kays, R., Wikelski, M., & Bohrer, G. (2012). Moderating argos location errors in animal tracking data. *Methods in Ecology and Evolution*, *3*, 999–1007.

Dujon, A. M., Lindstrom, R. T., & Hays, G. C. (2014). The accuracy of Fastloc-GPS locations and implications for animal tracking. *Methods in Ecology and Evolution*, *5*, 1162–1169.

Duong, T. (2007). ks: Kernel density estimation and kernel discriminant analysis for multivariate data in r. *Journal of Statistical Software*, *21*, 1–16.

Fleming, C. H., Fagan, W. F., Mueller, T., Olson, K. A., Leimgruber, P., & Calabrese, J. M. (2015). Rigorous home range estimation with movement data: A new autocorrelated kernel density estimator. *Ecology*, *96*, 1182–1188.

Gardner, B., McClintock, B. T., Converse, S. J., & Hostetter, N. J. (2022). Integrated animal movement and spatial capture–recapture models: Simulation, implementation, and inference. *Ecology*, *103*, 1–13.

Gimenez, O., Choquet, R., & Lebreton, J. D. (2003). Parameter redundancy in multistate capture-recapture models. *Biometrical Journal*, *45*, 704–722.

Grace, J. B., Anderson, T. M., Seabloom, E. W., Borer, E. T., Adler, P. B., Harpole, W. S., Hautier, Y., Hillebrand, H., Lind, E. M., Pärtel, M., Bakker, J. D., Buckley, Y. M., Crawley, M. J., Damschen, E. I., Davies, K. F., Fay, P. A., Firn, J., Gruner, D. S., Hector, A., ... Smith, M. D. (2016). Integrative modelling reveals mechanisms linking productivity and plant species richness. *Nature*, *529*, 390–393. https://doi.org/10.1038/nature16524

Hammond, P. S., Francis, T. B., Heinemann, D., Long, K. J., Moore, J. E., Punt, A. E., Reeves, R. R., Sepúlveda, M., Sigurosson, G. M., Siple, M. C., Víkingsson, G., Wade, P. R., Williams, R., & Zerbini, A. N. (2021). Estimating the abundance of marine mammal populations. *Frontiers in Marine Science*, *8*, 735770.

Hooten, M. B., Schwob, M. R., Johnson, D. S., & Ivan, J. S. (2023). Geostatistical capture-recapture models. *arXiv preprint*, arXiv:2305.04141. https://doi.org/10.48550/arXiv.2305.04141

Hostetter, N. J., Gardner, B., Sillett, T. S., Pollock, K. H., & Simons, T. R. (2019). An integrated model decomposing the components of detection probability and abundance in unmarked populations. *Ecosphere*, *10*, e02586.

Ivan, J. S., White, G. C., & Shenk, T. M. (2013). Using auxiliary telemetry information to estimate animal density from capture-recapture data. *Ecology*, *94*, 809–816.

Jarrett, C., Haydon, D. T., Morales, J. M., Ferreira, D. F., Forzi, F. A., Welch, A. J., Powell, L. L., & Matthiopoulos, J. (2022). Integration of mark–recapture and acoustic detections for unbiased population estimation in animal communities. *Ecology*, *103*, 1–9.

Johnson, D. S., London, J. M., Lea, M. A., & Durban, J. (2008). Continuous-time correlated random walk model for animal telemetry data. *Ecology*, *89*, 1208–1215.

Jolly, G. M. (1965). Explicit estimates from capture-recapture data with both death and immigration-stochastic model. *Biometrika*, *52*, 225–248.

Kéry, M., & Schaub, M. (2012). *Bayesian Population Analysis using WinBUGS: A hierarchical perspective*. Academic Press.

Kranstauber, B., Cameron, A., Weinzerl, R., Fountain, T., Tilak, S., Wikelski, M., & Kays, R. (2011). The movebank data model for animal tracking. *Environmental Modelling and Software*, *26*, 834–835.

Lesser, M. R., & Brewer, S. (2012). How sampling affects estimates of demographic parameters. *Journal of Vegetation Science*, *23*, 1170–1179.

Lindenmayer, D. B., & Likens, G. E. (2010). The science and application of ecological monitoring. *Biological Conservation*, *143*, 1317–1328.

London JM. 2020. *pathroutr: An r package for (re-)routing paths around barriers*.

Mahaffy, S. D., Baird, R. W., Harnish, A. E., Cullins, T., Stack, S. H., Currie, J. J., Bradford, A. L., Salden, D. R., & Martien, K. K. (2023). Identifying social clusters of endangered main Hawaiian islands false killer whales. *Endangered Species Research*, *51*, 249–268.

Marsh, H., & Sinclair, D. F. (1989). Correcting for visibility bias in strip transect aerial surveys of aquatic fauna. *The Journal of Wildlife Management*, *53*, 1017–1024.

Martien, K. K., Taylor, B. L., Chivers, S. J., Mahaffy, S. D., Gorgone, A. M., & Baird, R. W. (2019). Fidelity to natal social groups and mating within and between social groups in an endangered false killer whale population. *Endangered Species Research*, *40*, 219–230.

McClintock, B. T., Abrahms, B., Chandler, R. B., Conn, P. B., Converse, S. J., Emmet, R. L., Gardner, B., Hostetter, N. J., & Johnson, D. S. (2022). An integrated path for spatial capture–recapture and animal movement modeling. *Ecology*, *103*, 1–21.

Morales, J. M., Moorcroft, P. R., Matthiopoulos, J., Frair, J. L., Kie, J. G., Powell, R. A., Merrill, E. H., & Haydon, D. T. (2010). Building the bridge between animal movement and population dynamics. *Philosophical Transactions of the Royal Society, B: Biological Sciences*, *365*, 2289–2301.

Nichols, J. D., & Williams, B. K. (2006). Monitoring for conservation. *Trends in Ecology & Evolution*, *21*, 668–673.

Norris, J. L., & Pollock, K. H. (1996). Nonparametric MLE under two closed capture-recapture models with heterogeneity. *Biometrics*, *52*, 639–649.

Oleson, E. M., Boggs, C. H., Forney, K. A., Hanson, M. B., Kobayashi, D. R., Taylor, B. L., Wade, P. R., & Ylitalo, G. M. (2010). *Status review of Hawaiian insular false killer whales* (Pseudorca crassidens) *under the endangered species act*. https://repository.library.noaa.gov/view/noaa/3752

Petrovskaya, N., Petrovskii, S., & Murchie, A. K. (2012). Challenges of ecological monitoring: Estimating population abundance from sparse trap counts. *Journal of the Royal Society Interface*, *9*, 420–435.

Plummer, M. (2003). Jags: A program for analysis of bayesian graphical models using gibbs sampling. *Proceedings of DSC 2003*.

Plummer, M. (2018). *rjags: Bayesian graphical models using MCMC*. R package version 4-8.

R Core Team. (2020). *R: A language and environment for statistical computing*. https://www.r-project.org/

Reed, M. J., & Blaustein, A. R. (1997). Biologically significant population declines and statistical power. *Conservation Biology*, *11*, 281–282.

Rosenbaum, P. R. (1991). Discussing hidden bias in observational studies. *Annals of Internal Medicine*, *115*, 901–905.

Royle, J. A., Fuller, A. K., & Sutherland, C. (2016). Spatial capture–recapture models allowing markovian transience or dispersal. *Population Ecology*, *58*, 53–62.

Schaub, M., & Abadi, F. (2011). Integrated population models: A novel analysis framework for deeper insights into population dynamics. *Journal of Ornithology*, *152*, S227–S237.

Schaub, M., Gimenez, O., Sierro, A., & Arlettaz, R. (2007). Use of integrated modeling to enhance estimates of population dynamics obtained from limited data. *Conservation Biology*, *21*, 945–955.

Schorr, G. S., Baird, R. W., Hanson, M. B., Webster, D. L., McSweeney, D. J., & Andrews, R. D. (2009). Movements of satellite-tagged Blainville's beaked whales off the Island of Hawai'i. *Endangered Species Research*, *10*, 203–213.

Seber, G. A. F. (1965). Note on the multiple-recapture census. *Biometrika*, *52*, 249–260.

Sharma, R. K., Jhala, Y., Qureshi, Q., Vattakaven, J., Gopal, R., & Nayak, K. (2010). Evaluating capture-recapture population and density estimation of tigers in a population with known parameters. *Animal Conservation*, *13*, 94–103.

Sibly, R. M., & Hone, J. (2002). Population growth rate and its determinants: An overview. *Philosophical Transactions of the Royal Society, B: Biological Sciences*, *357*, 1153–1170.

Soisalo, M. K., & Cavalcanti, S. M. (2006). Estimating the density of a jaguar population in the Brazilian Pantanal using camera-traps and capture-recapture sampling in combination with GPS radio-telemetry. *Biological Conservation*, *129*, 487–496.

Sollmann, R., Gardner, B., & Belant, J. L. (2012). How does spatial study design influence density estimates from spatial capture-recapture models? *PLoS One*, *7*, e34575.

Thompson, W. L. (2004). *Sampling rare or elusive species: Concepts, designs, and techniques for estimating population parameters*. Island Press.

Tourani, M. (2022). A review of spatial capture–recapture: Ecological insights, limitations, and prospects. *Ecology and Evolution*, *12*, 1–13.

Watanabe, S. (2010). Asymptotic equivalence of Bayes cross validation and widely applicable information criterion in singular learning theory. *Journal of Machine Learning Research*, *11*, 3571–3594. http://arxiv.org/abs/1004.2316

Yoccoz, N. G., Nichols, J. D., & Boulinier, T. (2001). Monitoring of biological diversity in space and time. *Trends in Ecology & Evolution*, *16*, 446–453.

Zipkin, E. F., Inouye, B. D., & Beissinger, S. R. (2019). Innovations in data integration for modeling populations. *Ecology*, *100*, 1–3.

Zipkin, E. F., & Saunders, S. P. (2018). Synthesizing multiple data types for biological conservation using integrated population models. *Biological Conservation*, *217*, 240–250. https://doi.org/10.1016/j.biocon.2017.10.017

How to cite this article: Badger, J. J., Johnson, D. S., Baird, R. W., Bradford, A. L., Kratofil, M. A., Mahaffy, S. D., & Oleson, E. M. (2024). Incorporating telemetry information into capture-recapture analyses improves precision and accuracy of abundance estimates given spatiotemporally biased recapture effort. *Methods in Ecology and Evolution*, *15*, 1847–1858. https://doi.org/10.1111/2041-210X.14408